RESEARCH PAPER

Sustainable Synthesis of Carbon Dots from Bottle Gourd Peel and Development of Folic Acid–Scopoletin Nanoplatform for Antibacterial Therapy

Jeya Jeyamani [*1], Suguna Rajendran [2], and Renuka Radhakrishnan [3]

[1*]Department of Microbiology V. V. Vanniaperumal College for Women, Virudhunagar - 626001, Tamil Nadu, India.
[2]Department of Biotechnology , Madura College, Madurai - 625011, Tamil Nadu, India.
[3]Department of Biochemistry , V. V. Vanniaperumal College for Women, Virudhunagar - 626001, Tamil Nadu, India.

Abstract
The production of environmentally sustainable CDs from domestic solid waste was achieved using Lagenaria siceraria peel as a carbon source. The resulting CDs exhibited typical UV-Visible absorption characteristics, with maxima at 401.30 nm and 614.95 nm. These correspond to the π–π and n- π transitions, respectively. Hydroxyl group, carbonyl, and C –O functional groups were established from the FTIR spectra of the synthesized CDs, while an amorphous graphitic structure was shown using X-ray diffraction (XRD) with the broad peak occurring at 2θ of 24.78. Scanning electron microscopy (SEM) revealed spherical particles with a uniform distribution, ranging in size from 4 to 10 nm. The zeta potential of CDs was -32.2 mV. Scopoletin was isolated from the leaves of Simarouba glauca by methanol extraction and subsequent chromatographic separation. The presence of phenolics, flavonoids, tannins, carbohydrates, and proteins was confirmed using phytochemical analysis. Further confirmation of the coumarin structure of the extracted scopoletin was carried out using GC/MS and NMR spectroscopy. The functionalization of CDs was performed via EDC/NHS conjugation, and the FA-CDs were then conjugated with scopoletin to produce the FA-CDs-Sc conjugate. UV-Visible spectrum analysis showed two bands corresponding to the scopoletin structure at 202.1 nm and 362.7 nm. From FTIR spectra, successful attachment of scopoletin to the CDs was confirmed, with no change in the general structural framework. FA-CDs-Sc had a zeta potential value of -20.7 mV. The particle size obtained from dynamic light scattering analysis was 38.3 nm, with a PDI of 0.427. The novelty of this study lies in the integration of green-synthesized biomass-derived CDs with a naturally isolated bioactive compound and folic acid targeting ligand to develop a multifunctional antimicrobial nanoplatform. FA-CDs-Sc conjugates exhibited good antimicrobial activity on *Pseudomonas aeruginosa* (16 mm) and *Candida albicans* (17 mm).

Keywords: Carbon dots, Bottle gourd peel, Scopoletin, Folic acid, Antibacterial therapy, Nanoplatform
How to cite this article: Jeyamani J, Rajendran S, Radhakrishnan R. Sustainable Synthesis of Carbon Dots from Bottle Gourd Peel and Development of Folic Acid–Scopoletin Nanoplatform for Antibacterial Therapy. Int J Drug Deliv Technol. 2026;16(50s): 801-816. DOI: 10.25258/ijddt.16.50s.84

1. Introduction

The fast pace of nanotechnology development significantly impacted the synthesis of functional nanomaterials applicable in biomedicine and the environment. Among others, carbon dots (CDs) stand out as a class of carbon-based nanomaterials with unique optical properties, high biocompatibility, good chemical stability, and low toxicity (Ayanda et al., 2024). They display bright, tunable photoluminescence and are thus well-suited for biomedical applications such as bioimaging, sensing, drug delivery, and antibacterial agents. Still, traditional approaches to developing CDs are not sustainable, as they involve hazardous reagents, extreme reaction conditions, and excessive energy consumption (Barhoum et al., 2023).

Recently, green synthesis methodologies using natural biomass have attracted significant attention from researchers as environmentally friendly, cost-effective, and sustainable approaches for the synthesis of carbon dots (Usman & Cheng, 2024). Agricultural and food waste, such as fruit and vegetable peels, are abundant sources of carbonaceous substances, including carbohydrates, cellulose, and lignin, and can serve as efficient precursors for the synthesis of carbon nanomaterials (Jeevanandam & Danquah, 2025). Regarding the present study, Lagenaria siceraria (bottle gourd) peel is a valuable biomass source for the synthesis of green CDs.

Nanomaterials have a great potential for biomedicine; nevertheless, plant-origin bioactive compounds have also been widely studied (Chaachouay et al., 2023). For instance, Simarouba glauca is well known for its high therapeutic activity, attributed to multiple chemical constituents, including phenolics and coumarins (Jose et al., 2020). One such compound is scopoletin, a natural coumarin derivative with demonstrated antimicrobial, antioxidant, and anti-inflammatory effects (Sakthivel et al., 2022). Still, the practical application of such phytoconstituents is hindered by their relatively poor solubility, stability, and bioavailability. Nanocarrier-based systems offer the solution to these problems.

In addition to nanomaterials' modification, it is possible to enhance the applicability of CDs by functionalizing their surfaces with targeting ligands (Wang et al., 2023). For example, folic acid (FA) is a common component used to enhance the delivery of nanomaterials to targeted sites, namely those with overexpressed folate receptors, found in microbial cells and various cancers (Serag et al., 2024). Moreover, loading bioactive molecules, such as scopoletin, onto the surface of functionalized CDs may yield additional benefits.

*Author for Correspondence:Jeya Jeyamani

Despite many studies focused on the synthesis of CDs from biomass and their functionalization for biomedical applications, relatively little attention has been paid to fabricating CDs from biomass waste, combined with naturally occurring phytochemicals and targetable ligands, into a multifunctional nanoplatform (Usman & Cheng, 2024). Most often, efforts are dedicated to developing nanoparticles from biomass waste and to drug loading. At the same time, no attempt is made to explore the synergy among green synthesis, isolation of bioactive phytochemicals, and drug targeting.

In view of the previous knowledge, the purpose of the current study involves the development of a green and multifunctional nano-platform by preparing carbon dots using the peel of pumpkin Lagenaria siceraria, isolating scopoletin from Simarouba glauca, and forming folic acid functionalized CDs-scopoletin nano-conjugates (FA-CDs-Sc). Their physicochemical characteristics and potential antimicrobial effects have also been assessed for certain selected bacteria and fungi.

The novelty current work is the inclusion of the three major components, namely, CDs prepared through the green route from biomass waste, bioactive isolated compound from plant material such as scopoletin, and ligands like folic acid into a single nano-conjugate system. Such an approach would not only facilitate the use of waste biomass to produce valuable nanoparticles but also potentiate the therapeutic potential of phytochemicals through nanodelivery and targeting.

2. Materials and Methods

2.1. Materials

Fresh bottle gourd (Lagenaria siceraria) peels were obtained at a local vegetable market in Virudhunagar, Tamil Nadu, India, and were utilized as a carbon precursor (renewable). The source of Scopoletin was fresh leaves of Simarouba glauca.

Folic acid (FA), N-(3-dimethylaminopropyl)N-ethylcarbodiimide hydrochloride (EDC), and N-hydroxysuccinimide (NHS) were obtained from Sigma-Aldrich (USA). Ethanol, methanol and sodium hydroxide (NaOH) were taken as received. All conjugation studies were done in phosphate-buffered saline (PBS, pH 7.4).

Purification was carried out using dialysis membranes (MWCO 1000 Da). Silica gel (60–120 mesh) and pre-coated TLC plates (Silica gel 60 F254, Merck, India) were used for chromatographic separation. All solutions were made in deionized water or distilled water. For antibacterial studies, Mueller-Hinton agar (MHA) was purchased from HiMedia Laboratories Pvt. Ltd. (Mumbai, India). Standard Gram-positive and Gram-negative bacterial strains were used. Analytical grade reagents were used without purification.

2.2. Preparation of Raw Material

The gourd peel collected was thoroughly washed with distilled water to remove dirt and surface impurities and allowed to dry at room temperature. The peels were washed and using domestic mixer grinder, the peels were ground into a fine paste.

2.3. Green Synthesis of Carbon Dots

The peel paste was then prepared and dissolved in distilled water and exposed to thermal treatment at 150 °C for 2 hours. After heating, the reaction mixture was allowed to cool at room temperature. The cooled solution was filtered using a clean tea filter to remove larger particles to obtain a clear filtrate.

The filtrate was then refluxed at 150 °C over a period of 2 hours then cooled. The solution was then centrifuged at 4500 rpm to eliminate the remaining impurities and larger aggregates, as outlined by Mohammad et al. (2025). The supernatant obtained was reacted with 1 N sodium hydroxide (NaOH) to enable stabilization of the nanoparticles.

A clear and bright yellow suspension of carbon dots was obtained, which exhibited green fluorescence under ultraviolet (UV) light, indicating the successful formation of fluorescent carbon dots.

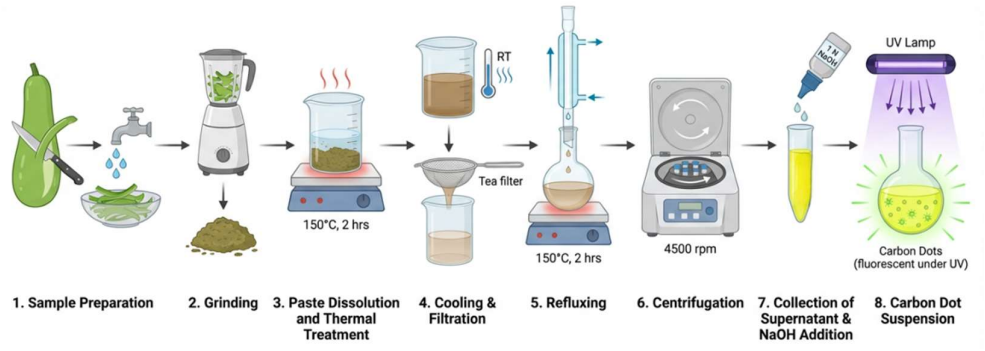

Fig.1. Schematic illustration of the experimental methodology for the green synthesis of carbon dots from bottle gourd peel, including raw material preparation, thermal treatment, filtration, reflux, centrifugation, and NaOH stabilization.

2.4. Isolation and Extraction of Scopoletin

The Leaves of Simarouba glauca were washed, dried in the shade, and ground into fine powder. The powdered material, weighing about 25 g, was Soxhlet-extracted with methanol for 6-8 h. A reduced-pressure filtered

extract was then concentrated to give a crude methanolic extract.

2.4.1. Qualitative Phytochemical Analysis

Qualitative phytochemical screening was performed to establish the occurrence or nonoccurrence of key secondary metabolites in the methanolic leaf extract of Simarouba glauca. The crude extract was made in methanol at a concentration of 10 mg/mL^{-1} and subjected to conventional qualitative assays.

Phytochemical constituents examined were alkaloids, saponins, flavonoids, phenols, tannins, carbohydrates, proteins, glycosides, steroids, terpenoids, and coumarins. The results were recorded as presence (+) or absence (−) based on the development of characteristic color changes or precipitates.

2.4.1.1. Detection of Alkaloids (Wagners Test)

The extract (1 ml) was mixed with 2 ml of 1% aqueous hydrochloric acid and heated in a steam bath. Wagner's reagent was then added in a few drops. The formation of a reddish-brown precipitate indicated the alkaloids.

2.4.1.2. Detection of Flavonoids (Alkaline Reagent Test)

One milliliter of the extract was mixed with 2 mL of 2% sodium hydroxide solution, resulting in a yellow coloration. The disappearance of color confirmed the presence of flavonoids upon the addition of dilute hydrochloric acid (Adegoke et al.,2010).

2.4.1.3. Detection of Phenols (Ferric Chloride Test)

One milliliter of extract was treated with 2 mL of 5% ferric chloride solution. The appearance of a blue-green coloration indicated the presence of phenolic compounds (Adegoke et al.,2010).

2.4.1.4. Detection of Tannins (Braymer's Test)

Two milliliters of extract was mixed with 3 mL of distilled water, followed by the addition of a few drops of 10% ferric chloride solution. The formation of a dark blue or greenish coloration indicated the presence of tannins (Adegoke et al.,2010).

2.4.1.5. Detectio'n of Saponins (Foam Test)

Three milliliters of extract were thoroughly shaken with 3 mL of distilled water. The appearance of stable foam or froth suggested the presence of saponins (Trease & Pharmacognsy, 1989).

2.4.1.6. Detection of Carbohydrates (Benedict's Test)

Benedict reagent was added to 2 mL of extract, and the mixture was heated in a water bath for 5 min. The formation of a reddish-brown precipitate indicated the presence of carbohydrates.

2.4.1.7. Detection of Proteins (Biuret Test)

Two milliliters of extract were mixed with 1 mL of sodium hydroxide solution and several drops of copper sulfate solution. Violet colouration formation indicated the presence of proteins.

2.4.1.8. Detection of Glycosides (Keller–Killiani Test)

Two milliliters of extract were mixed with glacial acetic acid containing a trace of ferric chloride, and then a drop or two of concentrated sulfuric acid was carefully added. The appearance of a brown ring at the interface also indicated the presence of glycosides (Harborne et al., 1998).

2.4.1.9. Detection of Steroids (Salkowski Test)

Chloroform was added to the 2 mL extract, and the mixture was mixed with concentrated sulfuric acid. The development of a reddish-brown colour indicated the presence of steroids (Adegoke et al., 2010)

2.4.1.10. Detection of Terpenoids (Salkowski Test)

The extract was combined with chloroform (5 mL), and concentrated sulfuric acid was added. A reddish-brown interface indicated the presence of terpenoids (Harborne et al., 1998).

2.4.2. Isolation and purification of scopoletin using chromatographic techniques

The stationary phase consisted of the crude extract placed on pre-coated analytical thin layer chromatography (TLC) aluminum plates (20 × 20 cm, Silica gel 60 F254, Merck, Mumbai, India). The mobile phase consisted of hexane: acetone in the ratio of 7:3 (v/v), which provided optimal separation of bands. The developed chromatograms were visualized under UV light at 254 nm (Sharma et al., 2019).

For further purification, column chromatography was carried out using a glass column (73 cm × 3 cm) packed with silica gel (60–120 mesh). This column was pre-equilibrated with hexane: acetone (7:3, v/v) and loaded with the crude extract. The same solvent system was used for elution. The eluents were collected and subjected to preparative TLC with the same solvent system. The purified compound was obtained by scraping the separated bands, eluting with solvent, and then filtering and concentrating the eluate.

2.4.3. Characterization of the Isolated Compound

A spectroscopic analysis was conducted on the methanolic leaf extract of Simarouba glauca to confirm the compound's structure. GC-MS was used to determine the molecular mass and fragmentation pattern of a compound. The obtained mass spectrum was compared with standard spectral databases to identify the compound.

2.5. Synthesis of Folic Acid-Conjugated Carbon Dots (FA-CDs)

The synthesis of folic acid-conjugated carbon dots (FA-CDs) was performed using a modification of the carbodiimide coupling procedure as described by Zhao et al. (2017). In brief, 20 mg of folic acid (FA) was dissolved in 8mL of 1× phosphate-buffered saline (PBS, pH 7.4) to give a clear yellow solution. This was followed by the addition of an aqueous solution of EDC (0.0260 g, 0.1356 mmol) and NHS (0.0156 g, 0.1355 mmol) to activate the carboxyl groups of FA.

The reaction mixture was sonicated at room temperature overnight to facilitate the formation of the active ester intermediate. This was followed by the addition of 2 mL of carbon dot (CD) solution (22 mg mL^{-1}), and the mixture was stirred continuously for 24 h to facilitate conjugation. The obtained solution was dialyzed (MWCO 1000 Da) to eliminate unreacted reagents and free FA. Finally, the purified FA-CDs were obtained as a yellowish powder after lyophilization.

2.6. Preparation of FA-CDs–Scopoletin Nanoconjugates

FA-functionalized carbon dots loaded with Scopoletin (FA-CDs–Sc) were prepared. Briefly, 1 mL of FA-CDs solution (8 mg mL^{-1}) was mixed with 1 mL of scopoletin solution (0.4 mg mL^{-1}, prepared in a suitable solvent system). The mixture was further diluted with 2 mL of phosphate-buffered saline (PBS, pH 7.4) to obtain a final reaction volume of 4 mL. The reaction mixture was stirred continuously at 25 °C (200 rpm) for 24 h to facilitate the interaction between FA-CDs and scopoletin via non-covalent interactions such as π–π stacking, hydrogen bonding, and electrostatic forces.

Following incubation, the solution was purified by dialysis using a membrane (MWCO 1000 Da) against 500 mL of deionized water for 2 h to remove unbound scopoletin and excess reagents. The purified FA-CDs–Sc nanoconjugate was then lyophilized for 48 h to obtain a dry powder for further characterization studies.

2.7. Characterization methods

The spectral and physicochemical properties of CDs and FA-CDs–Sc were investigated using multiple analytical techniques, including UV-vis spectroscopy, Fourier transform infrared (FTIR), X-ray Diffraction Analysis (XRD), Field Emisson Scanning Electron Microscopy (FE-SEM), Energy-Dispersive X-ray Spectroscopy (EDX) analysis, Transmission Electron Microscopy (TEM) and Zeta potential analysis. Ultraviolet-visible (UV-Vis) spectroscopy was conducted over 200-800 nm with a 1 cm quartz cuvette using a PerkinElmer UV spectrophotometer (USA). Fourier transform infrared (FTIR) was conducted in the wavelength range of 400-4000 cm^{-1}. (FE-SEM) was used to analyze the surface morphology of the synthesized carbon dots under high vacuum conditions with an accelerating voltage of 5-20 kV. A X'PERT PRO PANalytical, was used to perform X-ray diffraction (XRD) analysis with Cu Kα radiation (1.54 Å) over a suitable 2θ range. The additional morphological analysis and particle size determination were conducted using TEM. A zeta potential analyzer (Malvern Zetasizer Nano ZS, UK) was used to determine the surface charge and stability of the carbon dots. The fluorescence effect of the synthesized carbon dots was noted under UV light with the help of a UV transilluminator (365 nm).

2.8. Antibacterial Activity

The agar well diffusion method was used to test the antibacterial activity of the synthesized FA-functionalized carbon dots loaded with Scopoletin (FA-CDs–Sc) against *Staphylococcus aureus, Enterococcus faecalis*, *Pseudomonas aeruginosa*, *Escherichia coli* and *Candida albicans*. Mueller-Hinton agar was prepared and then sterilized. The chosen Gram-positive and Gram-negative bacteria strains were grown in nutrient broth and incubated at 37 °C for 18-24 h. The bacterial suspension was next adjusted to match the turbidity of a 0.5 McFarland standard.

The bacterial inoculum was uniformly spread on the agar plates using sterile cotton swabs. The agar plates were then drilled with wells about 6 mm in diameter using a sterile cork borer. Different concentrations (20, 40, and 60µg corresponds to II, III, and IV) of the test sample and ampicillin (I) as reference standard was loaded in the respective wells. The negative control was distilled water. The plates were incubated at 37 °C for 24 hrs. The antibacterial activity was then calculated from the zone of inhibition (in mm) in each well after incubation (Serag et al., 2024).

3. Result and Discussion

3.1. Green synthesis and visual observation of carbon dots

The CDs prepared from the peel extract of Lagenaria siceraria undergo a dramatic change from a turbid, brown precursor to a clear, yellow-colored product after thermal treatment and filtration, suggesting carbonization. The prepared CDs exhibited a strong green emission under ultraviolet illumination at 365 nm, indicating photoluminescence.

The fluorescence behaviour is due to quantum confinement and surface defect states, which are common in carbonaceous nanomaterials. Surface functional groups such as hydroxyl, carbonyl, and carboxyl groups present on CDs due to their biomass source play a significant role in determining the optical behavior of these nanoparticles (Shabbir et al., 2023). Using a natural carbon source offers the advantage of in-situ surface passivation without the need for exogenous passivators, thereby improving the fluorescence of CDs. The current investigation has successfully demonstrated the synthesis of CDs from the waste biomass by a green technique. CDs produced by these method exhibit optical properties similar to those of CDs obtained from other natural sources ((Usman & Cheng, 2024).

3.2. Isolation and Extraction of Scopoletin

3.2.1. Qualitative Phytochemical Analysis of Simarouba glauca

The qualitative screening for the methanolic leaf extract of S. glauca revealed the presence of several secondary metabolites (Table 1). Phenols, flavonoids, carbohydrates, tannins, and proteins were found in the extract, whereas the absence of saponins, alkaloids, glycosides, steroids, and terpenoids was noted.

Table 1. Qualitative phytochemical screening of Simarouba glauca leaf extract

S. No.	Class of Compounds	Results
1.	Phenols	+
2.	Saponins	-
3.	Flavonoids	+
4.	Carbohydrate	+
5.	Tannins	+
6.	Protein	+
7.	Alkaloid	-
8.	Glycosides	-
9.	Steroids	-
10.	Terpenoids	-

*(+) indicates the presence and (-) indicates the absence of the particular phytochemical.

The presence of phenolic compounds and flavonoids indicates significant antioxidant activity, given their known ability to neutralize free radicals and mitigate oxidative stress (Tumilaar et al., 2022). Also, the presence of tannins, another type of polyphenolic compounds, is associated with their antimicrobial and astringent activity due to protein precipitation and membrane permeability changes (Nassarawa et al., 2023).

The presence of carbohydrates and proteins suggests that primary metabolites are present in the plant, a prerequisite for the stability and bioavailability of the extract's phytoconstituents. The lack of alkaloids, glycosides, steroids, and terpenoids indicates a certain selective composition of phytoconstituents that affects their biological activity. In this context, it should be noted that phenolic compounds and flavonoids indicate the presence of coumarin derivatives such as scopoletin, which possess antimicrobial, anti-inflammatory, and antioxidant activity (Witaicenis et al., 2014).

3.2.2. Purification and characterization of scopoletin

The phytoconstituents in the methanolic extract of Simarouba glauca were separated using TLC and column chromatography. Based on the experiments, the best separation is achieved with a hexane: acetone ratio of 7:3, which provides the highest band resolution.

Several bands were observed in the TLC profiles under ultraviolet light (254 nm). The solvent front was observed to migrate to 4.5 cm, while the major fluorescent compound present in fraction giving an Rf of 0.67. Meanwhile, the standard compound corresponding to an Rf of 0.64. Since the Rf values of the isolated compound and standard compound are relatively close, the polarity is also expected to be the same (Fig.1 (a)).

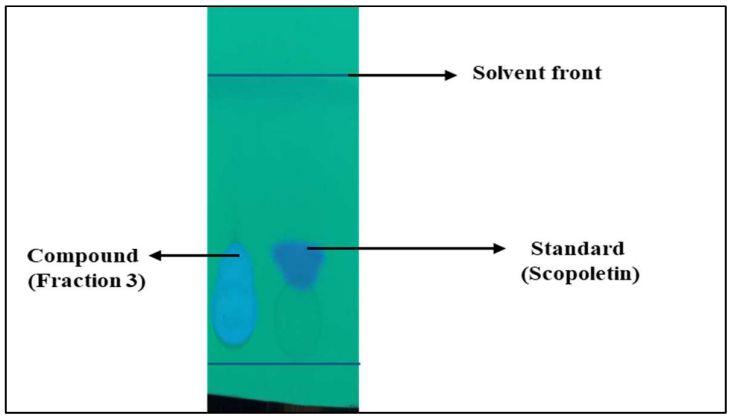

Fig. 1 (a). TLC profile of Simarouba glauca extract using hexane:acetone (7:3, v/v), showing compound (Rf = 0.67) and standard (Rf = 0.64) under UV light (254 nm).

In column chromatography, six fractions were obtained from the extracts, and fraction 3 was selected based on its visible fluorescence under UV exposure. This is due to the fluorescence characteristics arising from the extended conjugated π-electron structure of the coumarin derivative (Sundaramurthy et al., 2022). Using preparative TLC, a major compound was isolated. The presence of a single band indicates the compound's purity; it appears as a pale-yellow solid after extraction. The identity of the isolated compound was confirmed by GC–MS analysis.

GC-MS analysis was performed using the reference sample and Fraction 3 from the extraction of S. glauca to determine its chemical composition and the possible presence of scopoletin. The GC-MS chromatogram of the standard showed several peaks; specifically, a pronounced peak at 14.88 min was identified as scopoletin by comparison with library spectra (Fig. 1 (b), Table 2). The mass spectrum of the compound contained a molecular ion at m/z ≈ 192 and fragmentation patterns characteristic of coumarin derivatives (Lopez-Avila & Yefchak, 2011).

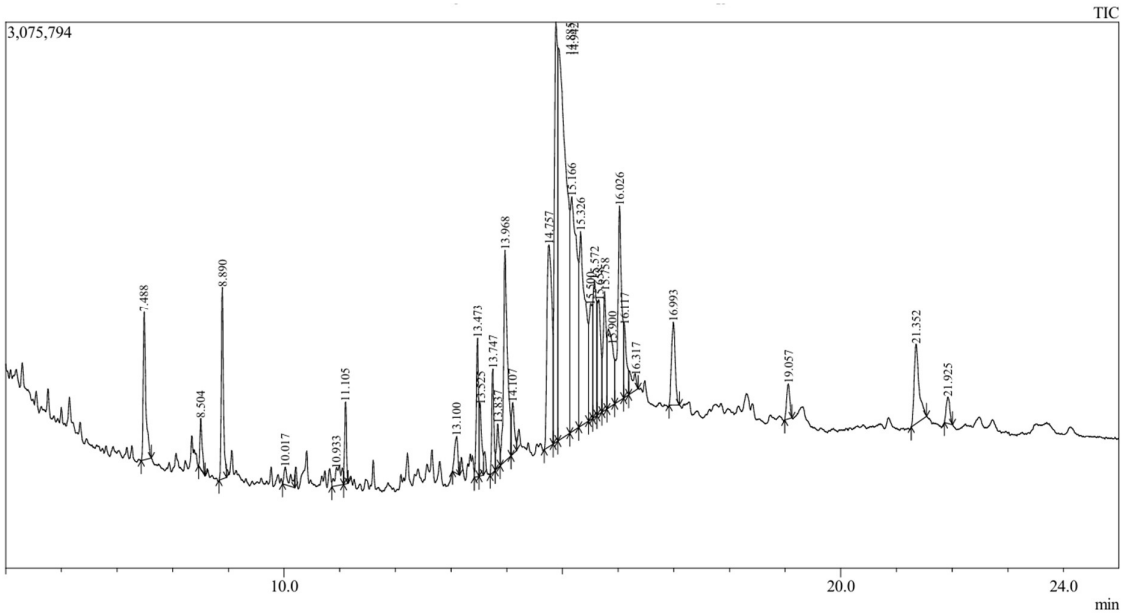

Fig. 1 (b). GC–MS chromatogram of standard showing a peak corresponding to scopoletin at RT ≈ 14.88 min.

Table 2. GC–MS analysis of standard sample

Peak No.	Retention Time (min)	Area (%)	Compound Name
1	7.488	2.49	Dodecanal
2	8.504	0.70	Dodecane, 4,6-dimethyl-
3	8.890	2.63	Phenol, 3,5-bis(1,1-dimethylethyl)-
4	10.017	0.56	1,2-Benzenedicarboxylic acid derivative
5	10.933	0.82	Nonadecane
6	11.105	0.98	Heneicosane
7	13.100	0.75	2-Bromododecane
8	13.473	1.94	Benzene derivative
9	13.525	1.15	Hexadecanoic acid methyl ester
10	13.747	1.38	Spiro compound
11	13.837	0.75	Octasiloxane derivative
12	13.968	5.39	n-Hexadecanoic acid
13	14.107	0.95	Dibutyl phthalate
14	14.757	6.51	Scoparone
15	**14.885**	**8.83**	**Scopoletin**
16	14.942	20.50	Tridecanal
17	15.166	9.90	1-Octadecanol
18	15.326	7.60	Octasiloxane
19	15.500	2.57	Heneicosane
20	15.572	2.92	Methyl stearate
21	15.658	2.65	Phytane
22	15.758	2.47	Silabicyclo compound
23	15.900	2.84	Oleic acid
24	16.026	4.99	Octadecanoic acid
25	16.117	1.26	Tetradecane
26	16.317	0.68	Docosanoic acid ethyl ester
27	16.993	1.94	Glutarimide derivative
28	19.057	0.70	Iron complex
29	21.352	2.52	13-Octadecenal
30	21.925	0.62	Siloxane derivative

In turn, the GC-MS chromatogram for Fraction 3 depicted several compounds, among which there was a large amount of aliphatic substances (Fig. 1 (c)). Notably, the peak obtained at RT ≈ 15.25 min coincides with scopoletin in terms of retention time and spectrum comparison with the peak from the reference sample (Table 3). Thus, it can be concluded about the existence of the compound in Fraction 3.

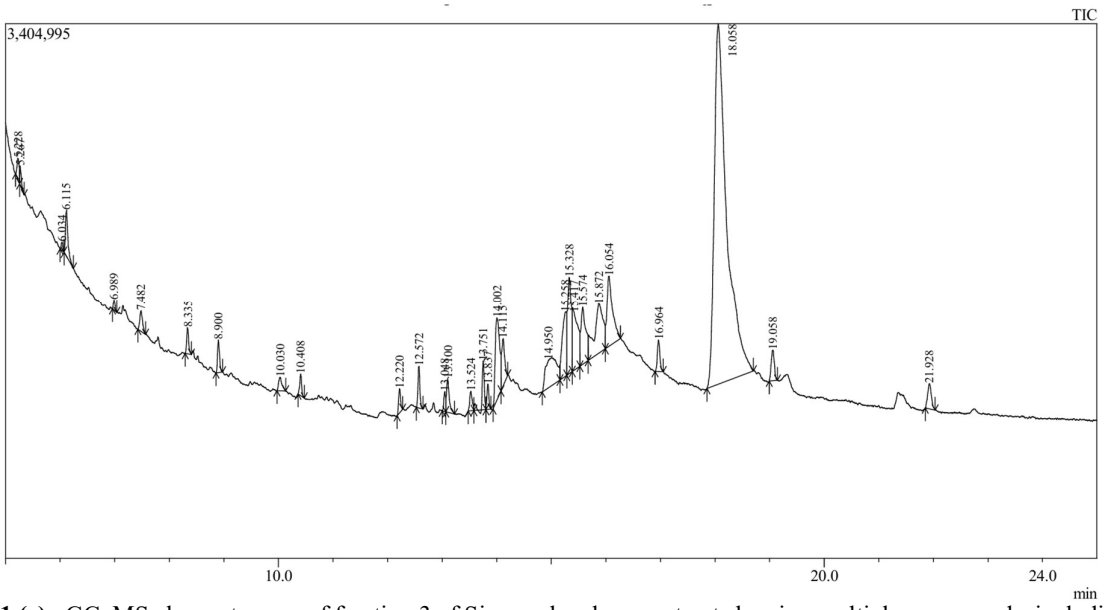

Fig. 1 (c). GC–MS chromatogram of fraction 3 of Simarouba glauca extract showing multiple compounds, including a peak corresponding to scopoletin at RT ≈ 15.25 min.

Table 3. GC–MS analysis of Fraction 3 of Simarouba glauca

Peak No.	Retention Time (min)	Area (%)	Tentative Compound
1	5.228	0.55	Siloxane derivative
2	5.267	0.30	Cycloheptasiloxane
3	6.034	0.15	Cyclotrisiloxane
4	6.115	1.23	Octasiloxane
5	6.989	0.20	Silane derivative
6	7.482	0.64	Dodecanal
7	8.335	0.59	Siloxane derivative
8	8.900	0.75	Phenolic compound
9	10.030	0.51	Diethyl phthalate
10	10.408	0.47	Benzoic acid derivative
11	12.220	0.58	Silicate compound
12	12.572	0.92	Alkene derivative
13	13.048	0.41	Alkyne compound
14	13.100	1.01	Phthalate ester
15	13.524	0.58	Fatty acid methyl ester
16	13.751	1.15	Spiro compound
17	13.837	0.56	Siloxane derivative
18	14.002	4.12	n-Hexadecanoic acid
19	14.115	1.71	Phthalate derivative
20	14.950	3.71	Scoparone
21	15.258	3.34	**Scopoletin (tentative)**
22	15.328	4.23	Siloxane derivative
23	15.417	3.68	Hydrazine derivative
24	15.574	3.21	Methyl stearate
25	15.872	5.17	Oleic acid
26	16.054	4.63	Octadecanoic acid
27	16.964	0.92	Siloxane derivative
28	18.058	**52.48**	**9-Octadecenamide (major compound)**
29	19.058	1.10	Siloxane derivative
30	21.928	1.08	Siloxane derivative

Alongside scopoletin, aliphatic compounds predominated in the examined fraction, with the peak area for 9-octadecenamide being the highest (52.48%). Other compounds identified included fatty acids (oleic acid and stearic/octadecanoic acid), esters, and phenolic derivatives (Patil & Murthy, 2020). This observation can explain the diversity of substances present in plant fractions, as many compounds can co-elute or even coexist within a single fraction. Thus, the concordance of retention times in the reference and Fraction 3

samples provides grounds for concluding that scopoletin is present in Fraction 3. In conclusion, GC-MS analysis confirmed the presence of scopoletin in Fraction 3 based on the coincidence of retention times and spectral similarities. The GC-MS results are consistent with previous findings on coumarins in medicinal plants (Shettar & Hiremath, 2025).

3.3. Synthesis of FA-CDs and FA-CDs–Sc nanoconjugates

FA conjugation to the surface of CDs has been achieved via carbodiimide coupling chemistry. In particular, the carboxylic groups in FA have been activated with N-(3-dimethylaminopropyl)-N'-ethylcarbodiimide hydrochloride (EDC) and N-hydroxysuccinimide (NHS), forming an active NHS ester. Then, the resulting NHS-ester-activated FA was reacted with surface amine groups on CDs, forming stable amide bonds and generating FA-functionalized CDs. Covalent coupling strategies are widely applied because of their efficient operation under mild aqueous conditions and ability to preserve the biological functionality of both ligands and nanoparticles (Bhattacharjee & Prasad, 2023).

FA conjugation to CDs renders the nanoparticles targeting ability because the ligand selectively recognizes folate receptors expressed in numerous cell types. Modification of the surface also increases dispersibility and functional possibilities of CDs, making them eligible for further drug loading (Yan et al., 2018). Next, scopoletin has been introduced to the surface of FA-CDs, forming FA-CDs-Sc nanoconjugates. The loading process was based on non-covalent interactions between scopoletin molecules and the FA-CD surface, including π-π interactions between the aromatic system of scopoletin and the graphitic structure of CDs, hydrogen bonding between hydroxyl and carbonyl groups, and electrostatic interactions among other functional groups on the particle surface. Non-covalent methods of nanoparticle loading have the advantage of preserving the structural integrity of the drug molecules and still providing an effective binding to the nanoparticle (Debnath & Srivastava, 2021).

3.4. Characterization Studies

3.4.1. Characterization of carbon dots (CDs)

3.4.1.1. UV-Vis spectroscopy

UV-Vis spectroscopy was used to assess the optical absorption properties of the synthesized carbon dots, and the spectrum as shown in Fig. 2. The absorption profile showed a strong peak at 401.30 nm and a secondary broad peak at 614.95 nm.The absorption peak at approximately 401 nm is commonly attributed to the π–π electronic transitions of aromatic C=C bonds within the sp^2-hybridized carbon core of the carbon dots (Arroyave et al., 2021). This confirms the formation of a graphitic carbon structure during thermal treatment. Such π–π transitions are one of the typical properties of carbon-based nanomaterials produced using biomass-based precursors.

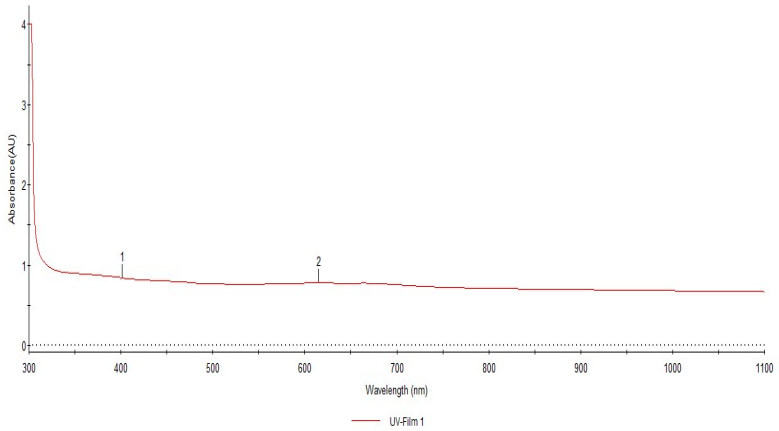

Fig.2. UV–Vis absorption spectrum of carbon dots synthesized from Lagenaria siceraria peel showing characteristic absorption peaks at 401.30 nm and 614.95 nm.

The broad absorption band observed around 614.95 nm can be associated with n–π transitions of surface functional groups, particularly those containing oxygen, such as carbonyl (C=O) and hydroxyl (–OH) groups (Devi & Luwang, 2025). These surface states are important determinants of the optical and electronic properties of carbon dots such as their fluorescence behaviour and interaction with biological systems.

Moreover, the comparatively wide and trailing absorption pattern into the visible range indicates the existence of surface defect states and non-homogenous energy levels, which are typical of green-synthesized carbon dots (Arroyave et al., 2021). The energy states that are caused by such defects increase light absorption and have applications in bioimaging and antimicrobial applications.

The optical characteristics of the observed material are in line with other reported works on biomass-derived carbon dots, where the combination of the core carbon structure with surface functionalization was the cause of similar absorption properties (Liu et al., 2020). The effective transformation of bottle gourd peel into

fluorescent carbon nanomaterial is proved by the successful formation of these optical signatures.

3.4.1.2. Fourier transform infrared spectroscopy (FTIR)

The surface functional groups on the synthesized carbon dots were analyzed by Fourier transform infrared (FTIR) spectroscopy; the spectrum is shown in Fig. 3. It exhibited multiple characteristic absorption bands, confirming the presence of oxygen-containing functional groups.

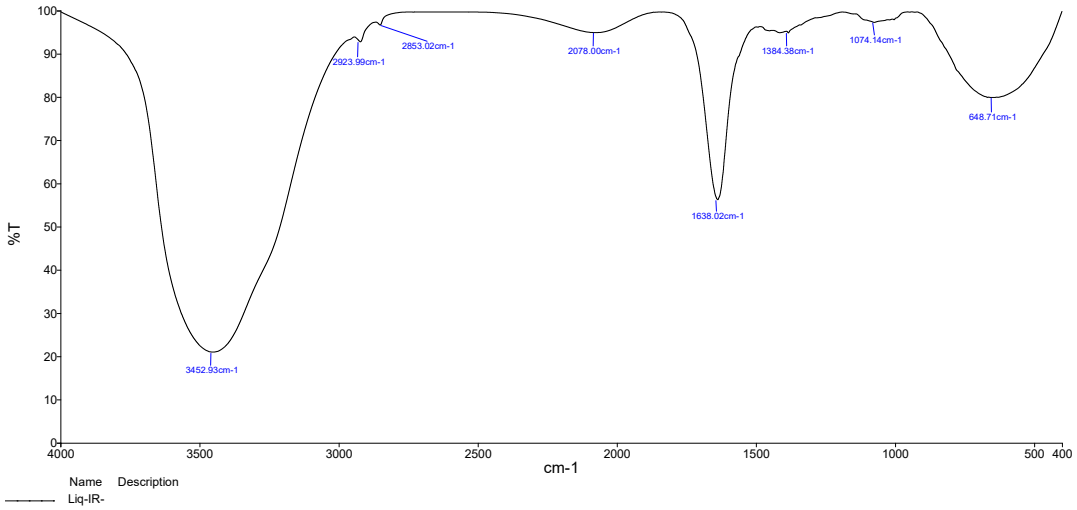

Fig.3. FTIR spectrum of carbon dots synthesized from Lagenaria siceraria peel

The appearance of a broad absorption peak at 3452.93 cm^{-1} is related to O-H stretching vibrations and this shows the presence of hydroxyl groups. These groups are typically associated with surface passivation and improved hydrophilicity of carbon dots prepared from biomass materials (Zaib et al., 2021).

C=C stretching vibrations of aromatic rings are observed at 1638.02 cm^{-1} and 1384.38 cm^{-1}, indicating the existence of sp^2 -hybridized carbon domains in the carbon core structure (Himaja et al., 2014). These aromatic domains play a crucial role in the creation of the conjugated carbon network that gives carbon dots its optical properties.

A clear peak at 1074.14 cm^{-1} corresponds to C-O stretching vibrations, indicating the presence of alcohol, ether, or carboxyl functional groups on the surface (Maddina et al., 2025). Functional groups also play an important role in enhancing the solubility and stability of nanoparticles in aqueous media. Moreover, the absorption at 648.71 cm^{-1} is attributed to C -H bending vibrations, which again proves that aliphatic carbon structures are present in the synthesized product (Yadav et al., 2020). In general, the FTIR results indicate that the synthesized carbon dots contain abundant surface functional groups, particularly oxygen-containing moieties, which are typical of green-synthesized carbon nanomaterials. These functional groups contribute to increased dispersion stability and provide active sites for potential interactions in biological systems.

3.4.1.3. Scanning Electron Microscopy (SEM) Analysis

Scanning electron microscopy (SEM) was used to analyze the surface morphology of the synthesized carbon dots (CDs) and the size distribution of these particles, as depicted in Fig. X(a–b). The micrographs demonstrate that the fabricated CDs have a dominant spherical structure and fairly uniform distribution throughout the substrate. The particles appear as bright, well-defined spots against a darker background, indicating good contrast and successful formation of nanoscale carbon structures.

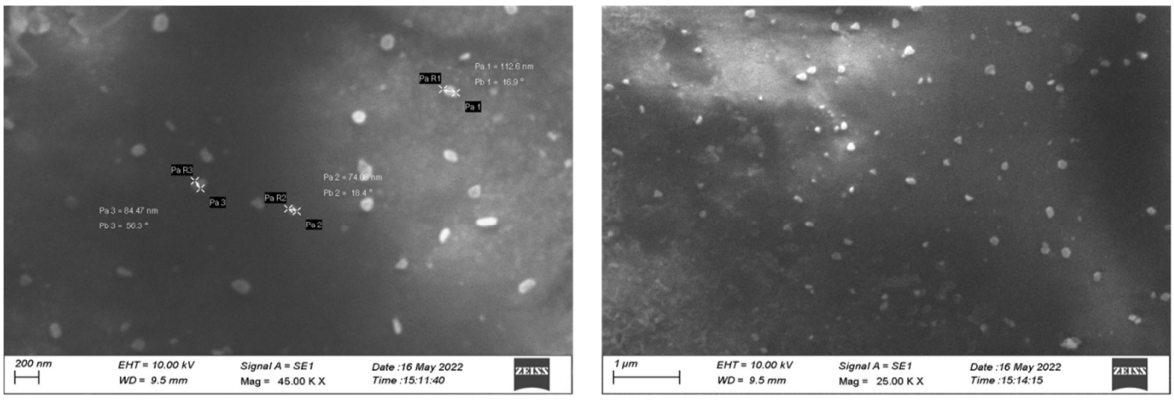

(a) **(b)**

Fig. 4. SEM micrographs of synthesized carbon dots: (a) high magnification (45.00 KX) showing spherical morphology with particle size in the range of 4–10 nm; (b) low magnification (25.00 KX) showing homogeneous dispersion of nanoparticles across the surface

Higher magnification (45.00 KX) reveals clearly defined nanoparticles and a size estimation indicates that the size of the synthesized CDs lies between 4-10 nm in diameter, indicating successful nanoscale production. There is no notable aggregation, which may be due to functional groups on the surface that stabilize the particles during synthesis through electrostatic or steric repulsion (Liu et al., 2017). However, slight clustering observed in certain regions could be due to solvent evaporation effects during sample preparation.

At lower magnification (25.00 KX), the SEM image shows a broader distribution of particles across the surface, confirming the homogeneous dispersion of CDs. The comparatively small size distribution also implies that the hydrothermal synthesis process was characterized by controlled nucleation and growth. The observed spherical morphology is consistent with previously reported carbon dots prepared from biomass precursors, and isotropic growth favours energetically favourable spherical morphologies (Nammahachak et al., 2022).

The development of uniformly distributed spherical CDs within the nanometer size indicates an efficient process of carbonization and passivation throughout the synthesis. This morphology is beneficial for drug delivery, bioimaging, and nanoemulsion systems due to its surface area and increased contact with biological environments. These findings are in good agreement with earlier studies, where carbon dots synthesized via hydrothermal methods exhibited spherical morphology with sizes below 10 nm (Harish et al., 2022). The morphology and size distribution were observed, indicating the successful synthesis of nanoscale carbon dots that could be used in future physicochemical and biological applications.

3.4.1.4. Transmission Electron Microscopy

The HR-TEM analysis results demonstrated that CDs were successfully synthesized from Lagenaria siceraria peel, with spherical shapes and good dispersion. The particle size ranges from 7.8 to 13.5 nm, with an average of about 9-10 nm. The high-magnification image shows nanoparticles with a slight lattice, suggesting a degree of graphitization of the carbon core. In addition, the low-magnification image suggests no or negligible aggregation (Fig. 5).

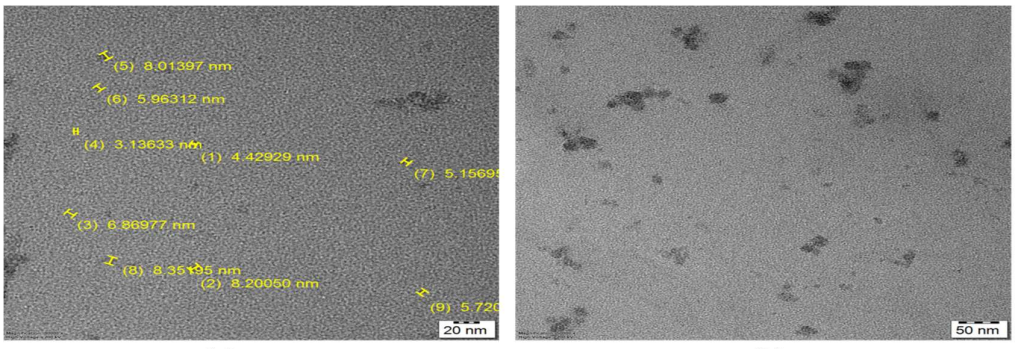

(a) **(b)**

Fig. 5. HR-TEM images of carbon dots (CDs) synthesized from Lagenaria siceraria peel at different magnifications: (a) high-resolution image (20 nm scale) showing spherical morphology and particle size distribution in the range of ~7.8–13.5 nm, and (b) low-resolution image (50 nm scale) illustrating uniform dispersion with mi
nimal aggregation.

The CDs' synthesis is explained by the fact that biomass components, such as cellulose and lignin,

undergo carbonization, which involves dehydration and polymerization reactions, producing nano-sized carbon cores with surface functional groups, such as hydroxyl and carboxyl groups, resulting in enhanced dispersibility and stability (Khairol et al.,2021). The CDs' dimensions and morphology are consistent with previous research on biomass-based CDs, ranging from 2 to 10 nm, with small differences arising from synthesis methods and conditions.

3.4.1.5. XRD Analysis

The XRD pattern of the synthesized carbon dots (CDs) shows a broad peak at 2θ ≈ 24.78°, corresponding to the (002) plane of graphitic carbon, indicating a disordered or turbostratic graphitic structure. Thus, the broadness of the characteristic peak indicates a low degree of crystallinity and small particle sizes, characteristic of CDs obtained from biomass.

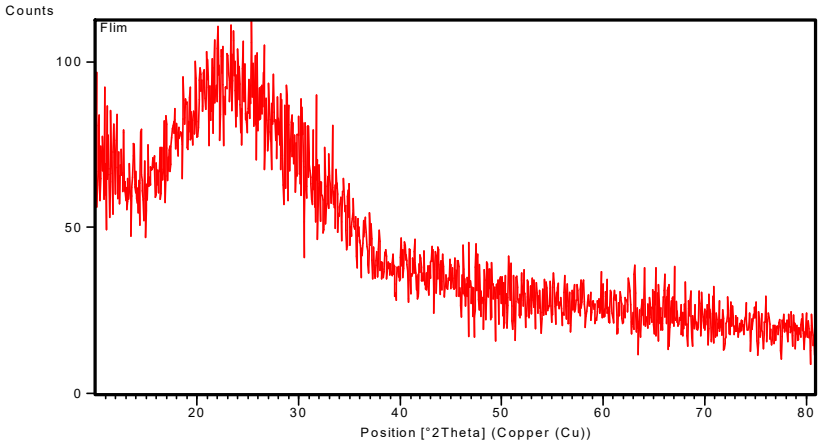

Fig.6. XRD pattern of CDs from Lagenaria siceraria peel

It is typical for biomass-derived CDs and carbonaceous nanoparticles to exhibit such broad diffraction bands in the 24-26° range (Zaib et al., 2022). A partially graphitic structure has been shown to improve the optical properties of carbon dots by forming active emission centers on their surfaces.

3.4.1.6. Zeta Potential Analysis

The zeta potential of the prepared Carbon Dots (CDs) was measured to determine the surface charge and colloidal stability of the nanoparticles. The test yielded an important result: a zeta potential of -32.2 mV, accompanied by an electrophoretic mobility of -0.000166 cm^2/Vs. The intensity distribution curve shows a well-defined, symmetrical peak near the mean, indicating a fairly homogeneous surface charge distribution among the particles (Karmakar, 2019).

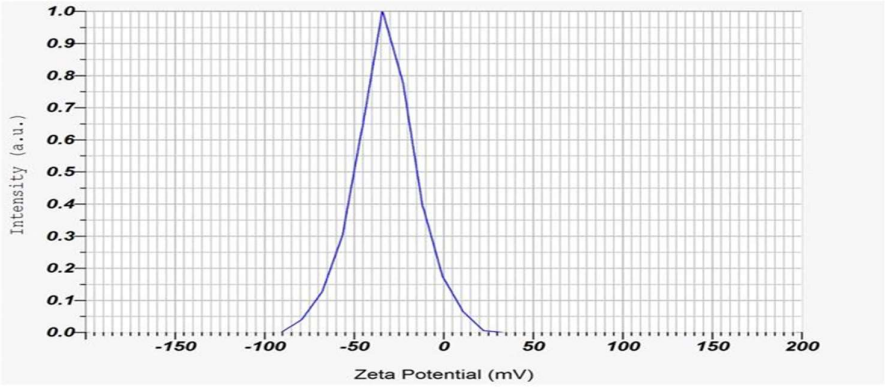

Fig.7. Zeta potential distribution of synthesized carbon dots in an aqueous dispersion.

Zeta potential values whose magnitude exceeds 30 mV indicate excellent colloidal stability (Midekessa et al., 2020). As such, a zeta potential value of -32.2 mV indicates that there is considerable electrostatic repulsion among the particles, thus ensuring that aggregation does not occur. A negative value of the surface charge usually indicates the existence of deprotonated functional groups, such as carboxyl ($-COO^-$) and hydroxyl ($-O^-$) groups, which create

repulsion forces to stabilize the nanoparticles (Gorohovs et al., 2025).

3.4.2. Characterization of FA-CDs–Sc nanoconjugates

To confirm that successful FA-CDs–Sc nanoconjugates had been obtained, various physicochemical analyses were performed. Based on UV-Vis spectroscopy, a characteristic absorption band was observed at 202.11 nm, indicating π–π electronic transitions in the carbon nanodots. Moreover, there were smaller bands at 362.71 nm due to n–π transitions of the organic surface-bound functional groups. These optical properties match those expected for well-passivated carbon dots containing heterogeneous electronic states (Tian et al., 2019).

Additionally, the materials' structure could be identified by FT-IR spectroscopy, which showed a broad vibrational band at 3311.93 cm^{-1}, assigned to O–H/N–H vibrations, and another at 1637.55 cm^{-1}, assigned to C=O (Amide I) vibrations. Taken together, the presented findings indicate a well-functionalized carbon surface that supports the attachment of Scopoletin and folate molecules.

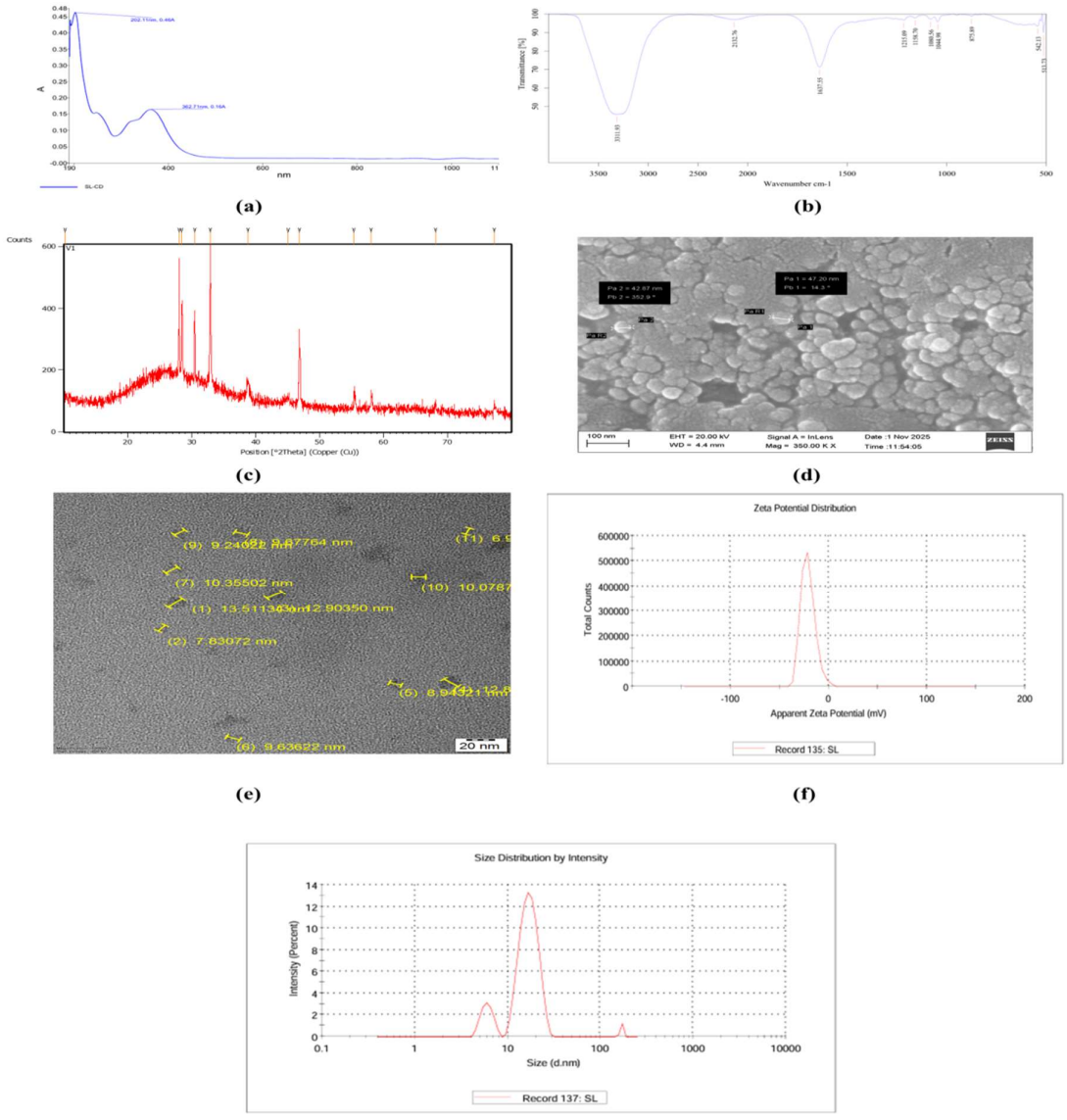

Fig.8. Characterization of FA-CDs–Sc nanoconjugates: (a) UV-Visible absorption spectrum; (b) FT-IR spectrum; (c) XRD pattern; (d) SEM micrograph; (e) High-resolution TEM image; (f) Zeta potential distribution; and (g) DLS size distribution by intensity.

To characterize the crystalline properties of FA-CDs–Sc nanoconjugates, X-ray diffraction analysis was performed. According to the XRD diffractogram, there was a characteristic halo visible at approximately $2\theta \approx 25°$, indicating the absence of a crystalline structure in carbon nanomaterials. However, the presence of sharp

diffraction peaks at 2θ ≈ 28°, 33°, 47°, and 58° indicates a crystalline phase in the nanoconjugates, possibly due to Scopoletin -containing components (Narayan et al., 2025).

Morphological analysis and colloidal stability were studied through the use of electron microscopy and dynamic light scattering (DLS) approaches. According to scanning electron microscopy (SEM) images, there are spherical nanoparticles with a surface diameter ranging from 42.87 to 47.20 nm. On the other hand, TEM images provided more detailed information about the inner structure of nanoparticles with core sizes that vary from 6.9 to 13.5 nm, having a representative core size of 9.24 nm. The difference between TEM-based core measurements and Z-average hydrodynamic diameter by DLS at 38.3 nm (PDI = 0.427) can be explained by solvation shell effect and the presence of FA ligand extending from the surfaces of nanoparticles in aqueous medium. Moreover, the nanoconjugates have a zeta potential of -20.7 mV, which is sufficient enough for achieving colloidal stability for biological purposes (Snee, 2018).

3.5. Antimicrobial activity of FA-CDs–Sc nanoconjugates

The antimicrobial activity of FA-CDs-Sc nanoconjugates was measured using the agar well diffusion method with selected microbial strains (Fig 9). The results showed that the test samples exhibited a dose-dependent increase in activity against all tested strains. The test sample had an activity zone of 14 mm against *Staphylococcus aureus*, compared with 19 mm against ampicillin. The same trend was observed in the case of *Escherichia coli*, where the activity was 15 mm, equal to the control. However, *Enterococcus faecalis* was less sensitive to the test samples, showing no activity at low doses and activity zones of 9-12 mm. Ampicillin, on the other hand, showed strong inhibition of 25 mm for this strain. In the case of *Pseudomonas aeruginosa*, the activity ranged from 12 to 16 mm for the test sample, whereas no activity zones were observed with ampicillin. Similar results were obtained for *Candida albicans*, with inhibition zones ranging from 12 to 17 mm, compared with 0 mm for ampicillin.

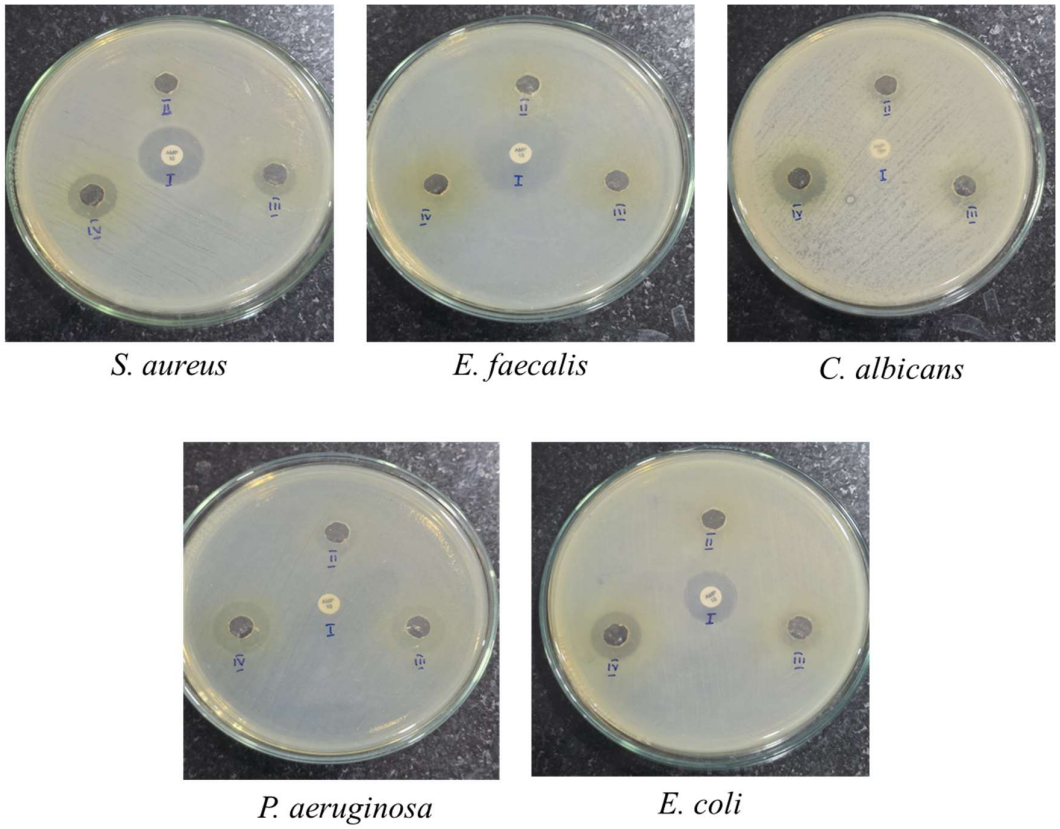

Fig. 9. Antibacterial activity assay plates of the synthesized nanoconjugates against test pathogens, demonstrating zones of inhibition.

The antimicrobial activity could be attributed to the synergistic properties of carbon dots and the loaded phytoconstituent. The carbon dots were known to cause membrane disruption and the formation of reactive oxygen species, leading to cellular damage, whereas conjugation and nanoscale structure ensured better penetration into microbial cells (Chen et al., 2026). The higher activity against Gram-negative bacterial pathogens, such as *Pseudomonas aeruginosa*, was possibly due to the ability of nanostructures to penetrate outer membrane structures that confer resistance to conventional antibiotics (Modi et al.,

2023). The higher antifungal activity against *Candida albicans* indicated the broad-spectrum activity of the test samples.

4. Conclusion

The present study employed an eco-friendly technique to fabricate fluorescent CDs from waste Lagenaria siceraria peel, thereby demonstrating the successful valorization of biomass. Fluorescent carbon dots were shown to be photoluminescent by UV-Vis spectroscopy, whereas FTIR analysis revealed sp^2 hybridization and the presence of oxygen-containing functional groups. The use of SEM, TEM, and XRD allowed the authors to characterize spherical nanoparticles with a size range of 4-13.5 nm, which exhibited partially graphitized and amorphous morphologies; additionally, the negative zeta potential (−32.2 mV) indicated the good stability of CDs. The analysis of phytoconstituents was performed using GC-MS, which confirmed the presence of scopoletin in Simarouba glauca Fraction 3. The FA-CDs–Sc nanoconjugates were successfully synthesized using non-covalent and carbodiimide functionalization methods, enabling effective incorporation of scopoletin onto CD surfaces. The results revealed high antifungal and antibacterial activity of the nanoconjugates, with the maximum inhibitory effect against *Candida albicans* and *Pseudomonas aeruginosa*. Such potent activity was achieved due to the CDs and scopoletin synergism and enhanced nanoscale cell interactions. Further research should focus on the possibility of applying such FA-CDs-Sc nanoconjugates in anticancer therapy, bioimaging, and other applications.

References

1. Ayanda, O. S., Mmuoegbulam, A. O., Okezie, O., Durumin Iya, N. I., Mohammed, S. A. E., James, P. H., ... & Badamasi, H. (2024). Recent progress in carbon-based nanomaterials: critical review. Journal of Nanoparticle Research, 26(5), 106. https://doi.org/10.1007/s11051-024-06006-2
2. Barhoum, A., Meftahi, A., Kashef Sabery, M. S., Momeni Heravi, M. E., & Alem, F. (2023). A review on carbon dots as innovative materials for advancing biomedical applications: synthesis, opportunities, and challenges. Journal of Materials Science, 58(34), 13531-13579. https://doi.org/10.1007/s10853-023-08797-6
3. Usman, M., & Cheng, S. (2024). Recent trends and advancements in green synthesis of biomass-derived carbon dots. Eng, 5(3), 2223-2263. https://doi.org/10.3390/eng5030116
4. Jeevanandam, J., & Danquah, M. K. (2025). Agricultural Waste-Derived Carbon Nanomaterials for Biomedical Applications. In Waste-Derived Carbon Nanostructures: Synthesis and Applications (pp. 213-232). Cham: Springer Nature Switzerland. https://doi.org/10.1007/978-3-031-75247-6_9
5. Chaachouay, N., Azeroual, A., Bencherki, B., Douira, A., & Zidane, L. (2023). Various metabolites and or bioactive compounds from vegetables, and their use nanoparticles synthesis, and applications. In Nanomaterials from Agricultural and Horticultural Products (pp. 187-209). Singapore: Springer Nature Singapore. https://doi.org/10.1007/978-981-99-3435-5_10
6. Jose, A., Kannan, E., & Madhunapantula, S. V. (2020). Anti-proliferative potential of phytochemical fractions isolated from Simarouba glauca DC leaf. Heliyon, 6(4). https://doi.org/10.1016/j.heliyon.2020.e03836
7. Sakthivel, K. M., Vishnupriya, S., Priya Dharshini, L. C., Rasmi, R. R., & Ramesh, B. (2022). Modulation of multiple cellular signalling pathways as targets for anti-inflammatory and anti-tumorigenesis action of Scopoletin. Journal of Pharmacy and Pharmacology, 74(2), 147-161. https://doi.org/10.1093/jpp/rgab047
8. Wang, H., Ai, L., Song, Z., Nie, M., Xiao, J., Li, G., & Lu, S. (2023). Surface modification functionalized carbon dots. Chemistry–A European Journal, 29(65), e202302383. https://doi.org/10.1002/chem.202302383
9. Serag, E., Helal, M., & El Nemr, A. (2024). Curcumin loaded onto folic acid carbon dots as a potent drug delivery system for antibacterial and anticancer applications. Journal of Cluster Science, 35(2), 519-532. https://doi.org/10.1007/s10876-023-02491-y
10. Mohammad Nejad Khiavi, N., Sowti Khiabani, M., Rezaei Mokarram, R., Hamishekar, H., & Samadi Kafil, H. (2025). Green synthesis of carbon quantum dots (CQDs) from butternut squash (Cucurbita moschata) peel waste: characterization, antibacterial and antioxidant activity. Biomass Conversion and Biorefinery, 15(12), 18133-18144. https://doi.org/10.1039/D5NA00813A
11. Harborne, A. J. (1998). Phytochemical methods a guide to modern techniques of plant analysis. springer science & business media.
12. Trease, G. E., & Evans, W. C. (1989). pharmacognosy. Brailliar Tiridel can. Acmillian publishers, 13, 28-32.
13. Adegoke, A. A., Iberi, P. A., Akinpelu, D. A., Aiyegoro, O. A., & Mboto, C. I. (2010). Studies on phytochemical screening and antimicrobial potentials of Phyllanthus amarus against multiple antibiotic resistant bacteria. International Journal of Applied Research in Natural Products, 3(3), 6-12.

14. Sharma, B., Dangash, A., & Pandya, N. (2019). Estimation of scopoletin content in commercially extracted leaves of medicinal herb Artemisia annua L. using HPTLC. Int J Pharmacogn, 6(8), 273-276. : http://dx.doi.org/10.13040/IJPSR.0975-8232.IJP.6(8).273
15. Zhao, X., Zhang, J., Shi, L., Xian, M., Dong, C., & Shuang, S. (2017). Folic acid-conjugated carbon dots as green fluorescent probes based on cellular targeting imaging for recognizing cancer cells. RSC advances, 7(67), 42159-42167. http://dx.doi.org/10.1039/C7RA07002K
16. Shabbir, H., Csapó, E., & Wojnicki, M. (2023). Carbon quantum dots: the role of surface functional groups and proposed mechanisms for metal ion sensing. Inorganics, 11(6), 262.
17. Tumilaar, S. G., Hardianto, A., Dohi, H., & Kurnia, D. (2024). A comprehensive review of free radicals, oxidative stress, and antioxidants: Overview, clinical applications, global perspectives, future directions, and mechanisms of antioxidant activity of flavonoid compounds. Journal of Chemistry, 2024(1), 5594386.
18. Nassarawa, S. S., Nayik, G. A., Gupta, S. D., Areche, F. O., Jagdale, Y. D., Ansari, M. J., ... & Alotaibi, S. S. (2023). Chemical aspects of polyphenol-protein interactions and their antibacterial activity. Critical Reviews in Food Science and Nutrition, 63(28), 9482-9505. https://doi.org/10.1080/10408398.2022.2067830
19. Witaicenis, A., Seito, L. N., da Silveira Chagas, A., de Almeida Junior, L. D., Luchini, A. C., Rodrigues-Orsi, P., ... & Di Stasi, L. C. (2014). Antioxidant and intestinal anti-inflammatory effects of plant-derived coumarin derivatives. Phytomedicine, 21(3), 240-246. https://doi.org/10.1016/j.phymed.2013.09.001
20. Sundaramurthy, C. B., Nataraju, C. P. K., & Krishnappagowda, L. N. (2022). Design, synthesis, structural analysis and quantum chemical insight into the molecular structure of coumarin derivatives. Molecular Systems Design & Engineering, 7(2), 132-157.
21. Lopez-Avila, V., & Yefchak, G. (2011). Mass spectral fragmentation studies of coumarin-type compounds using GC high-resolution MS. Open Anal. Chem. J, 5(1), 27-36. https://doi.org/10.2174/1874065001150100027
22. Patil, S., & Murthy, K. R. (2020). Phytochemicals, antioxidant profile and GCMS analysis of ethanol extract of Simarouba glauca seeds. https://doi.org/10.5530/ajbls.2020.9.57
23. Shettar, P. S., & Hiremath, M. B. (2025). GC-MS analysis and anti-oxidant activity of bioactive compounds of Simarouba glauca leaf extracts. Natural Product Research, 39(19), 5481-5490. https://doi.org/10.1080/14786419.2024.2344737
24. Bhattacharjee, K., & Prasad, B. L. (2023). Surface functionalization of inorganic nanoparticles with ligands: a necessary step for their utility. Chemical Society Reviews, 52(8), 2573-2595. https://doi.org/10.1039/D1CS00876E
25. Yan, F., Jiang, Y., Sun, X., Bai, Z., Zhang, Y., & Zhou, X. (2018). Surface modification and chemical functionalization of carbon dots: a review. Microchimica Acta, 185(9), 424. https://doi.org/10.1007/s00604-018-2953-9
26. Debnath, S. K., & Srivastava, R. (2021). Drug delivery with carbon-based nanomaterials as versatile nanocarriers: progress and prospects. Frontiers in Nanotechnology, 3, 644564. https://doi.org/10.3389/fnano.2021.644564
27. Arroyave, J. M., Ambrusi, R. E., Robein, Y., Pronsato, M. E., Brizuela, G., Di Nezio, M. S., & Centurión, M. E. (2021). Carbon dots structural characterization by solution-state NMR and UV–visible spectroscopy and DFT modeling. Applied Surface Science, 564, 150195. https://doi.org/10.1016/j.apsusc.2021.150195
28. Devi, S., & Luwang, M. N. (2025). Engineering luminescent carbon dot emission through surface state functional group via heteroatom doping and unveiling the effect of solvents. Langmuir, 41(22), 13751-13762. https://doi.org/10.1021/acs.langmuir.4c05002
29. Liu, Y., Zhu, C., Gao, Y., Yang, L., Xu, J., Zhang, X., ... & Zhu, Y. (2020). Biomass-derived nitrogen self-doped carbon dots via a simple one-pot method: Physicochemical, structural, and luminescence properties. Applied Surface Science, 510, 145437. https://doi.org/10.1016/j.apsusc.2020.145437
30. Zaib, M., Akhtar, A., Maqsood, F., & Shahzadi, T. (2021). Green synthesis of carbon dots and their application as photocatalyst in dye degradation studies. Arabian Journal for Science and Engineering, 46(1), 437-446. https://doi.org/10.1007/s13369-020-04904-w
31. Himaja, A. L., Karthik, P. S., Sreedhar, B., & Singh, S. P. (2014). Synthesis of carbon dots from kitchen waste: conversion of waste to value added product. Journal of fluorescence, 24(6), 1767-1773. https://doi.org/10.1007/s10895-014-1465-1
32. Maddina, S. K., & Kandru, A. (2025). Identification of Functional Groups and Chemical Profiling of Ipomoea parasitica Using FTIR Spectroscopy. IJCRT Research Journal| UGC

Approved and UGC Care Journal| Scopus Indexed Journal Norms, 15(3), 50912-50923. https://doi.org/10.5281/zenodo.15861025

33. Liu, X., Li, J., Huang, Y., Wang, X., Zhang, X., & Wang, X. (2017). Adsorption, aggregation, and deposition behaviors of carbon dots on minerals. Environmental Science & Technology, 51(11), 6156-6164. https://doi.org/10.1021/acs.est.6b06558
34. Nammahachak, N., Aup-Ngoen, K. K., Asanithi, P., Horpratum, M., Chuangchote, S., Ratanaphan, S., & Surareungchai, W. (2022). Hydrothermal synthesis of carbon quantum dots with size tunability via heterogeneous nucleation. RSC advances, 12(49), 31729-31733. https://doi.org/10.1039/D2RA05989D
35. Harish, V., Tewari, D., Gaur, M., Yadav, A. B., Swaroop, S., Bechelany, M., & Barhoum, A. (2022). Review on nanoparticles and nanostructured materials: Bioimaging, biosensing, drug delivery, tissue engineering, antimicrobial, and agro-food applications. Nanomaterials, 12(3), 457. https://doi.org/10.3390/nano12030457
36. Khairol Anuar, N. K., Tan, H. L., Lim, Y. P., So'aib, M. S., & Abu Bakar, N. F. (2021). A review on multifunctional carbon-dots synthesized from biomass waste: design/fabrication, characterization and applications. Frontiers in energy research, 9, 626549. | https://doi.org/10.3389/fenrg.2021.626549
37. Zaib, M., Akhtar, A., Maqsood, F., & Shahzadi, T. (2021). Green synthesis of carbon dots and their application as photocatalyst in dye degradation studies. Arabian Journal for Science and Engineering, 46(1), 437-446. https://doi.org/10.1007/s13369-020-04904-w
38. Karmakar, S. A. N. A. T. (2019). Particle size distribution and zeta potential based on dynamic light scattering: Techniques to characterize stability and surface charge distribution of charged colloids. Recent Trends Mater. Phys. Chem, 28, 117-159..
39. Midekessa, G., Godakumara, K., Ord, J., Viil, J., Lattekivi, F., Dissanayake, K., ... & Fazeli, A. (2020). Zeta potential of extracellular vesicles: toward understanding the attributes that determine colloidal stability. ACS omega, 5(27), 16701-16710. https://doi.org/10.1021/acsomega.0c01582
40. Gorohovs, M., & Dekhtyar, Y. (2025). Surface functionalization of nanoparticles for enhanced electrostatic adsorption of biomolecules. Molecules, 30(15), 3206. https://doi.org/10.3390/molecules30153206
41. Tian, X. T., & Yin, X. B. (2019). Carbon dots, unconventional preparation strategies, and applications beyond photoluminescence. Small, 15(48), 1901803. https://doi.org/10.1002/smll.201901803
42. Narayan, S., Nagpal, K., & Kumar, P. (2025). Polyphenol-conjugated polysaccharide nanoplatforms for enhanced therapeutic efficacy. Expert Opinion on Drug Delivery, 22(9), 1237-1255. https://doi.org/10.1080/17425247.2025.2514714
43. Snee, P. T. (2018). The role of colloidal stability and charge in functionalization of aqueous quantum dots. Accounts of Chemical Research, 51(11), 2949-2956. https://doi.org/10.1021/acs.accounts.8b00405
44. Chen, P., He, L. G., Zhai, H., Yan, X., Luo, K. L., Yuan, H. Q., ... & Sun, Y. (2026). Carbon dots in generation of reactive oxygen species for antibacterial therapy: Advances and challenges. Chemical Communications. https://doi.org/10.1039/D5CC07289A
45. Modi, S. K., Gaur, S., Sengupta, M., & Singh, M. S. (2023). Mechanistic insights into nanoparticle surface-bacterial membrane interactions in overcoming antibiotic resistance. Frontiers in Microbiology, 14, 1135579. https://doi.org/10.3389/fmicb.2023.1135579